Transactions of the **14th International Conference on Structural Mechanics in Reactor Technology** (SMiRT 14), Lyon, France, August 17-22, 1997 **H08/3**

Kinematic single surface global model for the seismic analysis of RC frames

Miramontes D., Merabet O., Reynouard J.M.
INSA Lyon, France

ABSTRACT

A plasticity-based global approach is proposed to simulate the nonlinear behaviour of RC frames subjected to earthquakes. The proposed beam section model is characterized by a unique yield surface (interaction diagram in 2D stresses space), a new kinematic hardening rule and a pre-calibrated uniaxial cyclic law (equivalent moment curvature relationship). The analysis/experiment comparisons show good agreement with experimental results and suggest a possible extension to more general spatial cases.

INTRODUCTION

Reinforced concrete frames are widely used for buildings placed in zones of high seismicity. The inelastic incursions imposed during earthquakes require efficient numerical methods to carry out a nonlinear analysis of the whole structure. This analysis is needed to identify correctly the cyclic degradation process and/or the imminent failure of the structural system. Local or semi-local methods have been successfully applied to describe the nonlinear behaviour of RC structures. Nevertheless, they remain expensive for the nonlinear dynamic analysis of complete structures as frames.

At global level (the size of elements are usually greater than 50 cm), the volume of calculations can be considerably reduced by simplified kinematic hypothesis and pre-integrated behavioural laws. The damage parameters are directly related to observed global results (e.g. stiffness degradation, cyclic strength reduction, pinching, etc.). As a result, a beam kinematic field and global behavioural laws (e.g. moment-curvature $M-\Phi$) predict the seismic behaviour of RC frames efficiently [1].

Most of the constitutive relations for these global models have been derived from experimental results from certain class of loading paths. Furthermore, the complexity of the overall involved phenomena has been eliminated by simplified models assuming a decoupled effect of normal force, shear and flexion. However, for more general load histories this assumption is not valid and leads to inaccurate and unreliable results. Within the framework of the theory of plasticity the dependence of the stresses on the history of the material and their interaction, hardening and degradation can be described by means of internal variables.

In this work, a plasticity-based approach for a RC beam section is formulated in generalized variables. It is characterized by an interaction diagram as yield function, a new kinematic hardening rule and a pre-calibrated uniaxial cyclic law defining the evolution of the hardening modulus. A limit analysis of the RC cross section is carried out to identify three positive and negative points for the uniaxial envelope Moment-Curvature curve (M-ϕ) and eight points for the interaction diagram Moment-Normal effort (M-N). Both models [1D (M-ϕ) and 2D (plasticity-based)] have been implemented in the general purpose program Castem2000 of the French Commission of the Atomic Energy (CEA) [2]. The numerical results show a good agreement with experimental observations. The uniaxial model and the 2D plasticity model are also compared. For a constant normal force or at negligible variation, the uniaxial approach remains more attractive. In contrast, for significant values of the axial force or for a non negligible variation, only the 2D model is able to predict the observed cyclic phenomena.

NEW KINEMATIC HARDENING RULE

Several kinematic hardening rules have been proposed in order to simplify the cyclic description of materials. For instance, in the kinematic rule proposed by Prager [3], the yield surface follows the direction of the normal pointing outwards the yielding surface at contact stress σ_c. The model proposed by Ziegler [4] leaves the normality rule as a direction parameter. In this case the direction of flow is given by the current kinematic center X and the contact stress σ_c. A different kinematic rule with a new direction of plastic flow is proposed by Mroz [5]. The translation of the yield surface lies on the line connecting two contact stress points which normal pointing outwards the yield surfaces have the same direction. The first point σ_c corresponds to the reached yielding surface, whereas the second one σ_{c+1} corresponds to the next yielding surface to be engaged.

In the presented models the direction of flow is independent of loading path. As it was noted by Jiang [6] the direction of the yield surface independent of the stress increment or the maintenance of the initial center leads to a poor estimation of cyclic behaviour which is more accentuated when non-proportional loadings are involved. In order to take into account the applied stresses in the direction of plastic flow, a new translation rule is proposed. In this case, the final position of the kinematic center lies on the line connecting the elastic trial stress σ^e and the updated kinematic center X.

EQUATIONS OF THE CONTINUOUS PROBLEM

The constitutive equations of the proposed model are :

$\dot{\varepsilon} = \dot{\varepsilon}^e + \dot{\varepsilon}^p$	Partition of strains	(1)
$\dot{\sigma} = D^e[\dot{\varepsilon} - \dot{\varepsilon}^p]$	Behavioural law	(2)
$\dot{\varepsilon}^p = \dot{\lambda}\dfrac{\partial f}{\partial \sigma}$	Normality rule	(3)
$\sigma^e = \sigma_o + D^e \dot{\varepsilon}$	Elastic predictor	(4)
$f(\sigma, X) = (M - \xi) - P(N - \psi) = 0$	Yield function	(5)
$\dot{f} = \dfrac{\partial f}{\partial \sigma} : \dot{\sigma} + \dfrac{\partial f}{\partial X} : \dot{X} = 0$	Consistency condition	(6)
$\dot{X} = C(\kappa)\left(\sigma^e - X\right)\dot{\lambda}$	Kinematic law	(7)

$\dot{\kappa} = \dot{\lambda}\Omega$	Equivalent plastic strain rate	(8)
$\Omega = \frac{1}{\tau}\sigma\frac{\partial f}{\partial \sigma}$	Plastic work equivalence	(9)
$C(\kappa) = \frac{d\tau}{d\kappa}$	Hardening modulus	(10)
$\dot{\lambda} = 0$ if $f(\sigma,X)<0$	Condition of elastic behaviour	(11)
$\dot{\lambda} \geq 0$ if $f(\sigma,X)=0$	Condition of plastic behaviour	(12)

Equation (1) assumes a partition of strains in an elastic part and a plastic part with $\varepsilon=(\varepsilon_m,\phi)$ where ε_m is the membrane strain and ϕ the curvature. The equation (2) represents the elastoplastic constitutive relationship, with the plastic strain rate (equation 3) given by the normality rule. This one is defined by the plastic multiplier $\dot{\lambda}$ and the gradient of the yield surface $\partial f/\partial \sigma$. The equation (4) gives the elastic predictor. The equation (5) corresponds to the yield function with generalized stress $\sigma=(M,N)$ and kinematic center $X=(\xi,\psi)$. The equation (6) ensures a null rate of the yield function. The proposed kinematic rule is given by the equation (7), where $C(\kappa)$ is the hardening modulus which depends on the cumulated plastic equivalent strain κ (equation 8). The evolution of the hardening modulus is controlled by equations (8), (9) and (10). These equations combine the biaxial stress state to an equivalent uniaxial cyclic law previously calibrated [1]. Finally, equations (11) and (12) identify the elastic and plastic states.

Plastic multiplier

To achieve an admissible stress state during a plastic load increment, the expressions (5) and (6) should be verified. In this way, the equations (3) and (7) applied in equation (6) lead to the scalar multiplier :

$$\dot{\lambda} = \frac{\frac{\partial f}{\partial \sigma}\dot{\sigma}}{C(\kappa)(\sigma^e - X):\frac{\partial f}{\partial \sigma}} \tag{13}$$

Effective stresses and strains

In order to define the evolution of the hardening modulus $C(\kappa)$, the plastic dissipation for the biaxial and uniaxial spaces wrote :

$$\dot{W}^p = \sigma\dot{\varepsilon}^p = \tau\dot{\kappa} \tag{14}$$

where σ=(M,N) is the biaxial stress state, $\dot{\varepsilon}^p = (\dot{\phi}^p, \dot{\varepsilon}_m^p)$ are the associated plastic strains rates. τ is the equivalent stress in the uniaxial state and $\dot{\kappa}$ is the associated equivalent strain rate. With regard on equations (3) and (13), the equation (9) is expressed as :

$$\Omega = \frac{(M-\xi)\frac{\partial f}{\partial M} + (N-\psi)\frac{\partial f}{\partial N}}{\tau(e)} \tag{15}$$

For a null and constant normal force $\tau(e)$=t coincides with the cracking moment of the equivalent moment-curvature relationship. τ depending on the eccentricity e represents the elastic limit which remains constant for a purely kinematic hardening. The cumulated equivalent strain is given by :

$$\kappa_{i+1} = \kappa_i + \dot{\kappa} \tag{16}$$

with κ_i the cumulated plastic strain in the previous converged state.

Yield Surface for the proposed model

In this work, the loading surface is expressed by a polynomial interpolation based on the interaction diagram of the RC cross section. Each direction is composed of two straight lines and a polynomial of fifth degree. The final size of the yield surface is evaluated in such a way that for a null normal force the elastic limit coincides with the cracking moment of the moment-curvature relationship. Symmetrical or no symmetrical cross sections can be treated accurately [2].

$$f_1(M,N) = M - p_1 * N - p_2 \tag{17a}$$

$$f_2(M,N) = M - p_3 * N^5 - p_4 * N^4 - p_5 * N^3 - p_6 * N^2 - p_7 * N - p_8 \tag{17b}$$

$$f_3(M,N) = M - p_9 * N - p_{10} \tag{17c}$$

RETURN MAPPING STRATEGY

The determination of plastic strains requires the knowledge of plastic multiplier $\dot{\lambda}$ and the gradient of the yield function $\partial f/\partial\sigma$ (plastic flow direction) evaluated at the converged stress point σ_c. However this point is unknown and an iterative procedure is needed. Generally an implicit Newton-Raphson method is applied. The yield function expressed as a new dependent function of the plastic multiplier rate $\dot{\lambda}$ leads to a different strategy : the yield function $f(\dot{\lambda})$ and the converged value of $\dot{\lambda}$ are simultaneously verified. This procedure was adopted in this work. The principal steps of the iterative process include :

1. For a stress increment (ΔM, ΔN), the yield function $f(\sigma, X_0)$ (see equation 5) is evaluated with $\sigma = (M^e, N^e)$ the elastic predictor and $X_0 = (\xi, \psi)$ the updated kinematic center.
2. If the yield function is not violated $f(\sigma^e, X) \leq 0$, the stress point elastically evaluated is correct. Internal variables are updated and loading process goes on (return to step 1). On the other hand if $f(\sigma^e, X) > 0$, the trial stress should be corrected (equ. 17) and hardening of the yield surface takes place (equ. 18) :

$$\sigma = \sigma_0 + \dot{\sigma}^e - \dot{\lambda} D^e \frac{\partial f}{\partial \sigma} \tag{17}$$

$$\dot{X} = C(\kappa)\left(\sigma^e - X\right)\dot{\lambda} \tag{18}$$

with

$$\frac{\partial f}{\partial \sigma} = \left(\frac{\partial f}{\partial M}, \frac{\partial f}{\partial N}\right)^T \tag{19}$$

where $\frac{\partial f}{\partial M} = \pm 1$ according to the sign of the moment stress M and

$$\partial f/\partial N = -\sum_{n}^{1} n\, p_i\, (N-\psi)^{n-1} \qquad (20)$$

with $i = n = 1$ for f_1; $i = 8-n$ and $n=5$ for f_2 and $i = 10-n$ and $n=1$ for f_3. Similar expressions can be defined for the negative functions.

Equations (17) and (18) bring $f(\sigma,X)$ directly dependent of $\dot{\lambda}$. To verify $f(\dot{\lambda})=0$, $\dot{\lambda}_i=0$ for the first iteration step. The iterative process involves :

a) $$\Delta\dot{\lambda}_{i+1} = \frac{-f(\dot{\lambda}_i)}{\dfrac{\partial f(\dot{\lambda}_i)}{\partial \dot{\lambda}_i}} \qquad (21)$$

b) $$\dot{\lambda}_{i+1} = \dot{\lambda}_i + \Delta\dot{\lambda}_{i+1} \qquad (22)$$

c) $f(\dot{\lambda})$ is evaluated

If $f(\dot{\lambda}) > TOL$ return to a)

If $f(\dot{\lambda}) \leq TOL$ continue to step 3 (tolerance $TOL = 10^{-10}$).

3. The stress point (σ,X) is correct and the plastic strain rate $\dot{\kappa}$ is evaluated by the equations (10) and (11). The cumulated plastic strain and the internal variables are updated.
4. Next load step (return to 1)

If plastic flow occurs in an intersection point with two violated yield functions :

$$\dot{\varepsilon}^{p} = \dot{\lambda}_1 \frac{\partial f_1}{\partial \sigma} + \dot{\lambda}_2 \frac{\partial f_2}{\partial \sigma} \qquad (23)$$

with f_1 and f_2 the involved yield functions.

NUMERICAL EXAMPLES

Two predictive analysis shows the capabilities of the proposed model. Non damaged cross sections have been assumed in both cases in order to verify the applicability of the model for simplified analysis of current complete structures.

Simple RC frame

The first example concerns a double built-in RC frame. Test set-up and geometric characteristics are given in [7]. Basic concrete parameters are : f'_c=23.1Mpa the compression strength and ε'_c=0.0021 the associated strain, E_c=23100Mpa the Young modulus. Steel properties are : f_y=332.3Mpa the yielding limit and E_s=220000Mpa the Young modulus. The applied vertical and horizontal loads increase simultaneously (radial loading path). Numerical results have been performed by two different approaches : the previously proposed uniaxial cyclic model (1D model) [1] and the present model (2D model). The first one needs the moment-curvature relationship with axial load included. However, initial pre-stress is considered null (the dead weight of beam has been neglected). Consequently, the moment-curvature relationship for beam and columns are the same for both approaches. In addition to the moment-curvature envelop curve, the present model needs the interaction diagram (M,N).

The lateral displacement-load relationship is compared with the numerical results (Fig. 1). Maximum capacity and ultimate displacement for both models are close to experimental results (Table 2). Nevertheless, a significant different behaviour is observed for each one. In the plasticity-based model the increase of the axial force induces in a first time an increase of stiffness which decreases when inelastic axial strains progress. Consequently, the predicted behaviour is more realistic.

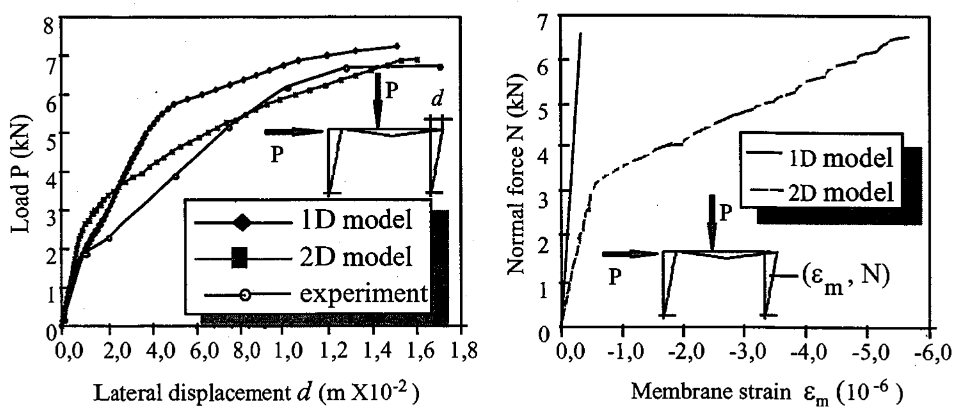

Fig. 1. Experimental vs. 1D/2D numerical results for a simple frame

Table 1. Comparison of load-lateral displacement

Response	Experiment	1D model (scatter)		2D model (scatter)	
Load P (kN)	68.0	72	(5.9%)	70	(2.9%)
Displacement. d (cm)	1.7	1.5	(-11.76)	1.6	(-5.9%)

The different behaviour can be explained by the description of the axial strain for both cases. For the uniaxial model this relationship is considered linear and decoupled of flexion. This behaviour is valid for the left column due to small stress applied. The lateral force produces an unloading of this member. The 2D model predicts a similar response. In contrast, the lateral force induces a high axial stress in the right column. Linear behaviour is not realistic. The 2D model takes into account the interaction between flexion and normal force and at the same time the nonlinear behaviour of axial strains (Fig. 1b). An averaged value of the total normal force during the construction of the envelop curve can not improve the results of the uniaxial model. In this example, the extreme variation of the normal force requires at least a 2D formulation integrating the interaction between flexion and axial force.

Four storey RC full scale frame

An experimental test on four storey full-scale RC frame was carried out in the European Laboratory for Structural Assessment at Ispra Joint Research Center in Italy. The structure has plan dimensions of 10 m x 10 m measured from column axis. Inter-storey heights are 3.5 m for ground storey and 3 m for subsequent stories. A solid slab with thickness of 0.15 m has been adopted for all stories. All members were detailed in accordance with Eurocode-8 rules (EC-8). Details of test setup and reinforced layout are reported in [8].

In order to define the experimental program, a set of artificial accelerograms were generated by using the waveforms derived from a real signal with a total duration of 10s. The amplitude of the signal corresponds to the peak nominal base acceleration equal 0.45g [8]. Torsional effects are not present in the global behaviour of the structure. Taking into account this behaviour only the interior frame has been modeled with 5 m of slab width.

The time history of storey displacements are shown in Figure 2. An important difference is found for maximal values due to the surestimation of lateral stiffness. The principal sources are : a) the assumed initial uncracked cross sections, b) the nonlinear unloading is not considered and c) the stiffening of the first floor du to axial load. The lateral displacement of the first level is not described correctly even if superior levels are more correctly simulated. The time history of frequencies remains close to observed values. Similarly, the time history of base-shear (Fig. 3) shows that the total lateral stiffness is in agreement with experimental results (Table 2).

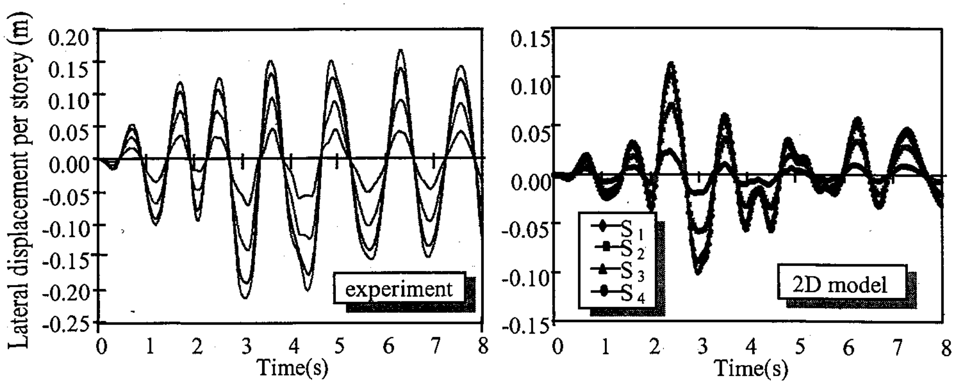

Fig. 2. Experimental/Numerical time history of lateral displacements per storey

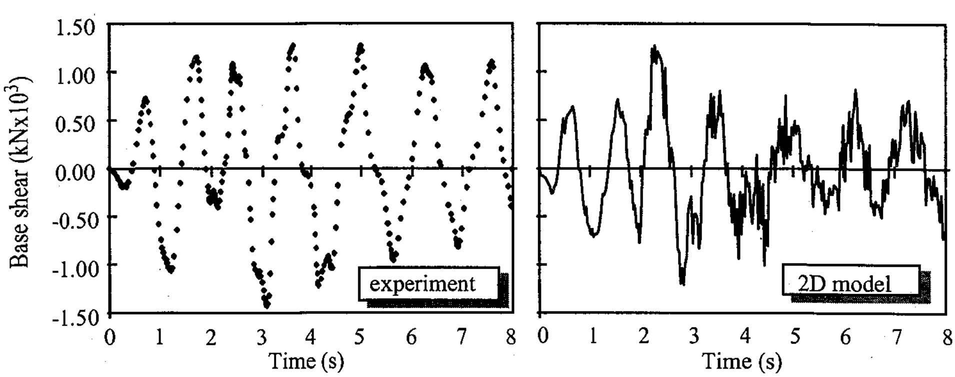

Fig. 3. Experimental/Numerical time history of base shear

It can be also observed that frequencies are well estimated. In depict of lateral displacement of first level, lateral forces for subsequent levels are well estimated (Table 3). Uncracked cross sections and axial force have produced one half of the observed displacement for the first floor. Nevertheless the global prediction of lateral forces and frequencies remains close to observed results.

Table 2. Comparison of global responses

Response	Experiment	2D model
D_{max} (cm)/time (s)	21.0/3.0	13.5/2.43
Base shear (kN)	1440	1337
Frequency (Hz)	0.820	0.913

Table 3. Maximum lateral forces (kN)

Force	Experiment	2D model	scatter %
F_1	5.78	10.42	80
F_2	5.77	5.9	2.25
F_3	5.38	5.77	7.25
F_4	6.72	6.0	-10.7

CONCLUSION AND PERSPECTIVES

The plasticity-based global model takes into account several phenomena considered as essentials for a correct description of RC frames. In a first time, the interaction of flexion and normal force is considered by a precise interaction diagram as yield function. In a second time, a new hardening law takes into account the increment of applied stress and finally, the evolution of hardening modulus is controlled by an uniaxial cyclic law previously calibrated. In the first exemple, the experimental/numerical comparison shows the importance of the interaction between flexion and axial force. The second one enhances the descriptive capabilities of the proposed model for the seismic analysis of complete frames. The model can be extended to spatial cases by using an interaction diagram defined by the normal force and two orthogonal moments (N, M_y, M_z) or a complete interaction for plane cases by a yield surface defined by the normal force, shear and moment (N, V, M)

REFERENCES

1. Miramontes, D., Merabet, O. and Reynouard, J. M. 1996. Beam Global Model for the Seismic Analysis for RC Frames. *Earth. Engrg. and Struct. Dyn.*, 25 : 671-688

2. Miramontes, D. 1996. Global model for the seismic analysis of RC frames: Phenomenological and Plasticity-based approches (in French). *Doctoral Dissert., INSA-Lyon.*

3. Prager, W. 1955. The theory of plasticity - a survey of recent achievements. *Proc. Instn. of Mech. Engrgs.* 169, 41-57. London, England.

4. Ziegler, H. (1959). A modification of Prager's hardening rule. *Quarterly of Appl. Mathematics*, 17 : 55-65.

5. Mroz Z. 1969. An attempt to describe the behaviour of metals under cyclic loads using a more general workhardening model. *Acta Mecanica*, 7 : 199-212.

6. Jiang, W. 1994. Study of two-surface plasticity theory. *J. Engrg. Mechanics, ASCE, 120* : 2179-2200.

7. Bertero, V. V. and McClure, G., 1964. Behaviour of R/C frames subjected to repeated reversible loads. Journal of American Concrete Institute, No. 10, 61 : 1305-1330.

8. Negro, P., Verzeletti, G., Magonette, G. E. and Pinto A. V. 1994. Tests on a four storey full-sacle R/C frame designed according to Eurocodes 8 & 2. Report EUR 15879 EN, Preliminary Report, ISPRA (Italy).